RESEARCH ARTICLE

EFFECT OF CRYSTAL SIZE ON THE OPTIMUM TEMPERATURE FOR THE HIGHEST CAPACITY OF A TREE-DIMENSIONAL POLYCRYSTALLINE SILICON SOLAR CELL

Moussa Camara[1], Moustapha Thiame[2], Mamoudou Touré[1], Haba Siba[1] and Ousmane Fanta Camara[1]

1. UniversitéGamal Abdel Nasser de Conakry Facultéé des Sciences BP: 1147 - Conakry République de Guinée.
2. Laboratoire de Chimie et de Physique des Matériaux (LCPM), Département de Physique, UFR ST, BP 523, Ziguinchor, Senegal.

…….....

Manuscript Info	*Abstract*
…………………….	………………………………………………

In this work, we have proposed a method for determining the optimum temperature of an n+-p-p+ single-face silicon photocell under polychromatic front illumination using Fossum's temperature-dependent diffusion coefficient model Dn (T). The capacitance is therefore determined as a function of temperature and the x and y dimensions of the crystal. The optimum temperature Topt that gives the best short-circuit capacitance is determined from the profile of the logarithm of capacitance versus the logarithm of temperature for different grain sizes.

…….....

Introduction:-
The performance of solar cells depends on several parameters intrinsic to the material, such as the thickness of the base [1], the doping rate [2], the diffusion coefficient [3], the lifetime [4], the diffusion length [5], the grain size [6-7-8], recombination at the junction [6-7-8], at the back [9], at the interfaces (Sg) [6-7-8] and the technology used to manufacture them. But also the natural parameters of the photocell exposure environment, such as the magnetic field [10], the magnetic field and temperature [11-12-13], the temperature [14, 15], the electric field [16], the irradiation [17], the irradiation energy flux [18], the solar concentration [19] and the variation in the angle of incidence [20] also have a strong influence on the conversion efficiency. Conversion efficiency is the perceptible indicator of the performance and comparability of solar cells. As this variable depends on all the factors and parameters that make up the solar cell, it is important to know what influences them.

Some papers have used one-dimensional models [14, 15] to determine the optimum temperature.

The aim of this work is to make a complementary contribution to the work already carried out on controlling the behaviour of the multi-crystal solar cell under the impact of temperature for three-dimensional models.

It is based on the study of temperature, capacity and grain size. The optimum temperature corresponding to the maximum short-circuit capacity is determined for several grain sizes.

Model and assumptions
Our study focuses on an n+/p/p+ polycrystalline solar cell under multicolour front illumination. For the three-dimensional modelling, we started from Fick's first law in one dimension, giving the number of electrons diffusing per unit of time and volume, which we generalised to three dimensions (Figure 1). From this generalised law in three

Corresponding Author:-Moussa Camara
Address:-UniversitéGamal Abdel Nasser de Conakry Facultéé des Sciences BP : 1147 - Conakry République de Guinée.

443

dimensions, we determined the diffusion current density, assuming that the solar cell is not polarised. We therefore considered a columnar model [21] (Figure 1) in which each grain of the crystal is assumed to have a regular parallelepiped shape.
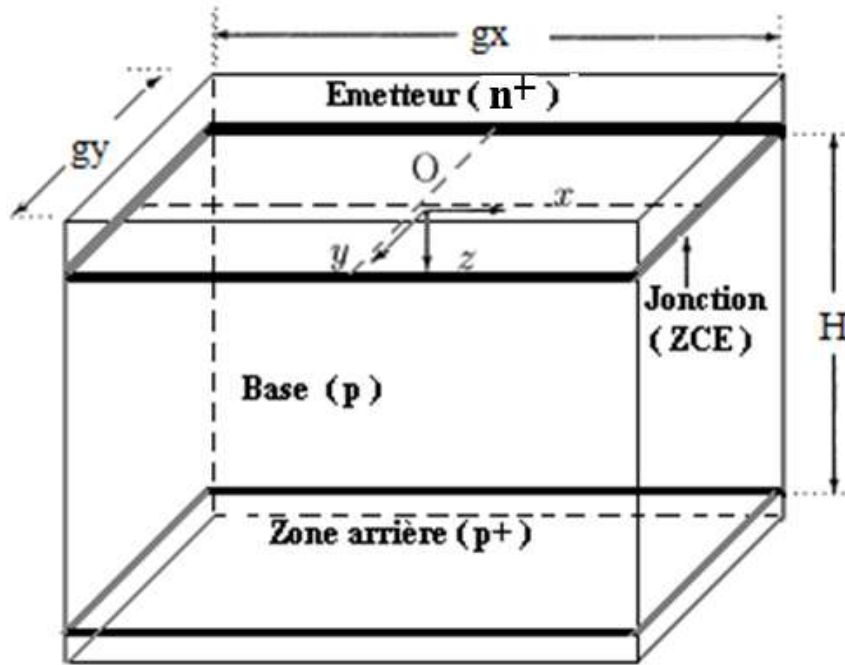
Figure 1:-Diagram of a grain of silicon crystal.

The continuity equation for photogenerated minority carriers in the base is:

$$\frac{\partial^2 \delta n(x, y, z)}{\partial x^2} + \frac{\partial^2 \delta n(x, y, z)}{\partial y^2} + \frac{\partial^2 \delta n(x, y, z)}{\partial z^2} - \frac{\delta n(x, y, z)}{Ln(T)^2} = -\frac{G(z)}{Dn(T)} \quad 1$$

$\delta n(x, y, z)$: minority electron flow.

Ln : electron scattering length in the base.

$$Ln(T)^2 = \tau \cdot Dn(T) \quad 2$$

Dn : is the electron diffusion coefficient in the base.

$$Dn(T) = \mu(T) \cdot \frac{k_b}{q} \cdot T \quad 3$$

$$\mu(T) = 1.43 \cdot 10^9 \cdot T^{-2.42} cm^2 \cdot V^{-1} \cdot s^{-1} \quad 4$$

$G(z)$:is the rate of generation of minority electrons in the base.

$$G(z) = \sum_{i=1}^{3} a_i \cdot \exp - b_i \cdot z \quad 5$$

ai and bi are determined from solar irradiance[18,22,23].
The solution to the continuity equation (1) is[18, 22]:

$$\delta n(x, y, z) = \sum_k \sum_j Z_{kj}(z) \cdot \cos(c_k \cdot x) \cdot \cos(c_j \cdot y) \quad 6$$

By replacing equation 6 in 1 and using the orthogonal conditions for cosine functions, we obtain the following continuity equation:

$$\frac{\partial^2 Z_{kj}(z)}{\partial z^2} - \frac{1}{L_{kj}^2} \cdot Z_{kj}(z) = -\frac{1}{D_{kj}} \cdot G(z) \quad 7$$

Avec $Z_{kj}(z) = A_{kj} \cdot \cosh\left(\frac{z}{L_{kj}}\right) + B_{kj} \cdot \sinh\left(\frac{z}{L_{kj}}\right) - \sum_{i=1}^{3} K_i \cdot \exp - b_i \cdot z \quad 8$

$$K_i = \frac{a_i L_{kj}^2}{D_{kj}\left(b_i^2 \cdot L_{kj}^2 - 1\right)} \quad 9$$

$$L_{kj} = \left[c_{kj}^2 + c_{kj}^2 + L_n^2(T)\right]^{-\frac{1}{2}} \quad 10$$

$$D_{kj} = \frac{Dn(T) \cdot \left[c_k \cdot g_x + \sin(c_k \cdot g_x)\right] \cdot \left[c_j \cdot g_y + \sin(c_j \cdot g_y)\right]}{16 \cdot \sin\left(c_k \cdot \frac{g_x}{2}\right) \cdot \sin\left(c_j \cdot \frac{g_y}{2}\right)} \quad 11$$

The boundaries that limit the base of the solar cell lead us to consider two boundary conditions that allow us to determine the expressions for A_{kj} and B_{kj} [6, 8, 18] :

✓   At the transmitter-base interface.

$$Dn \cdot \left[\frac{\partial \delta n(x,y,z)}{\partial z}\right]_{z=0} = Sf \cdot \delta n(x,y,z=0) \quad 12$$

✓   On the back.

$$Dn\left[\frac{\partial \delta n(x,y,z)}{\partial z}\right]_{z=H} = -Sb \cdot \delta n(x,y,z=H) \quad 13$$

Sf is the recombination velocity at the n+/p surface, which highlights the free charge flow that manages to cross the trqnsition zone.

Sb is the electron loss rate at the p/p+ interface, which represents the number of carriers lost by recombination at the back surface.

The boundary conditions taken at the contact surface between the grains of the crystal allow us to obtain the eigenvalues c_k and c_j [8, 18] :

$$Dn \cdot \left[\frac{\partial \delta n(x,y,z)}{\partial x}\right]_{x=\pm\frac{g_x}{2}} = \mp S_{gb} \cdot \delta n\left(\pm\frac{g_x}{2}, y, z\right) 14$$

$$Dn \cdot \left[\frac{\partial \delta n(x,y,z)}{\partial y}\right]_{y=\pm\frac{g_y}{2}} = \mp S_{gb} \cdot \delta n\left(x, \pm\frac{g_y}{2}, z\right) 15$$

Sg is the number of charges lost by recombination at the contact surface between the grains in cm.s^{-1}; g_x and g_y are the dimensions of the grains along the x and y axes. The signs $\pm$ come from the Cartesian reference point chosen at the centre of the crystal

Equation 6 in 14 and 15 gives the transcendental equations:

$$\tanh\left(c_x \cdot \frac{g_x}{2}\right) = \frac{Sg}{c_x \cdot D(Nb)} \quad 16$$

$$\tanh\left(c_j \cdot \frac{g_y}{2}\right) = \frac{Sg}{c_j \cdot D(Nb)} \quad 17$$

Choice of eigenvalues C_k and C_j

The values of C_k and C_j are obtained from the transcendental equations given by equations 16 and 17 by the graphical method or by programming.

We used the graphical method to extract the values of C_k and C_j. The functions $f(C_k)$ and $h(C_k)$ are plotted in the same frame of reference. The points of intersection of the curves of these two functions give the values of C_k and C_j. The crystal grain is assumed to be square, so $C_k = C_j$.

$$f(C_k) = \tanh\left(C_k \cdot \frac{g_x}{2}\right) \quad 18$$

$$h(C_k) = \frac{S_g}{C_k \cdot Dn(Nb)} \quad 19$$

Figure 2 shows the influence of temperature on the solutions C_k.
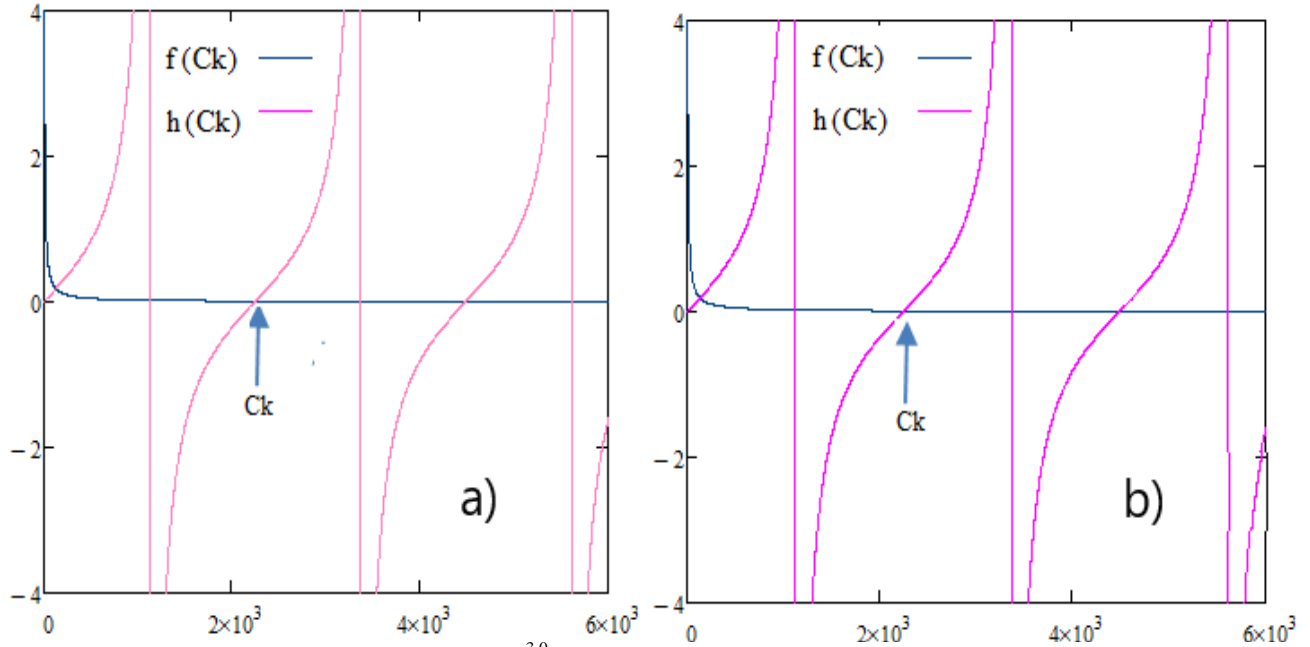
Figure 2:- Own values $S_g = 10^{3.0}$ cm/s, g = 20 μm, a)T = 273 K et b)T = 333 K

Variations in temperature and recombination rate at the interfaces (Sg) do not affect Ck values if $Sg \leq 10^{3.0}$ cm/s.

Tableau 1:- Own values C_k for $Sg = 10^{3.0}$ cm/s.

Temperature (K)	Own values $C_j = C_k$(/cm) ; j= 0, 1, 2, 3, 4				
273	127,613	2251,000	4492,000	6735,000	8978,000
333	127,613	2251,000	4492,000	6735,000	8978,000

These values are verified by several recombination velocities at grain interfaces sg $\leq 10^{3.0}$ cm/s and for different temperatures.
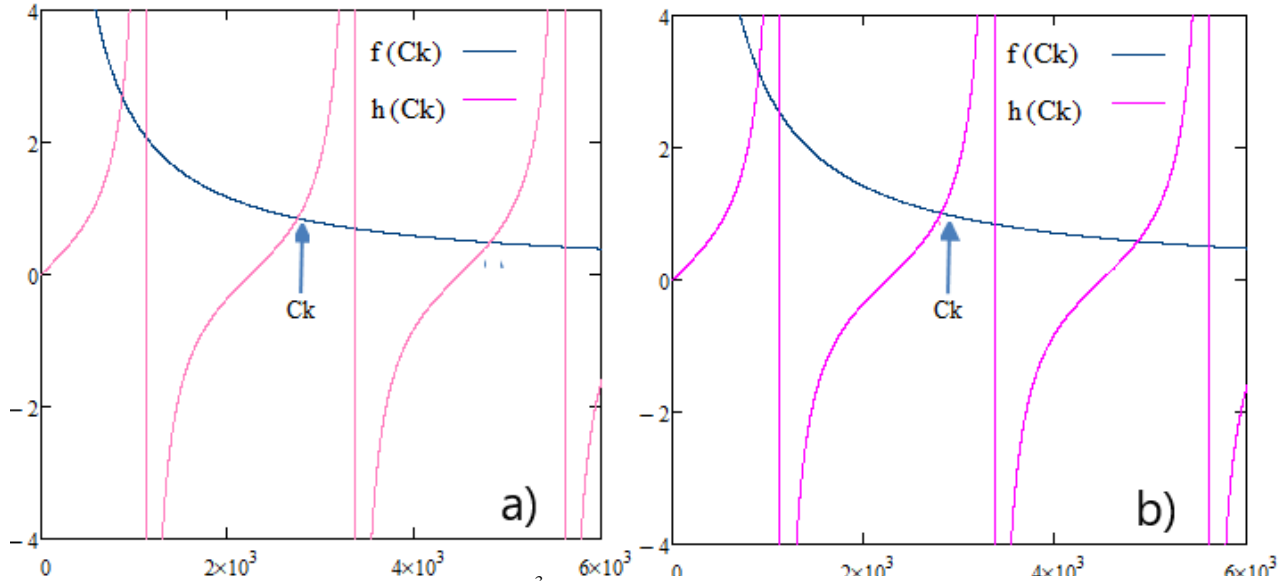
Figure 3: -Own values Sg> 10^3 cm/s, g = 20 µm, a) T = 273 K et b) T = 333 K.

Ck increases with temperature if Sg > 103.0 cm/s (Figure 3) as shown in Table 2.

Table 2: - Own values C_k for Sg = 5.10^4 cm/s.

Temperature (K)	Own values $C_i = C_k$ (/cm); k= 0, 1, 2, 3, 4				
273	867,635	2747,000	4811,000	6963,000	9154,000
333	916,425	2836,000	4891,000	7028,000	9208,000

In Figure 4, we will study the influence of grain size on the values of C_k and C_j. To do this, based on the above studies, we set the recombination velocity at the interfaces between two grains at $10^{3.0}$ cm/s.
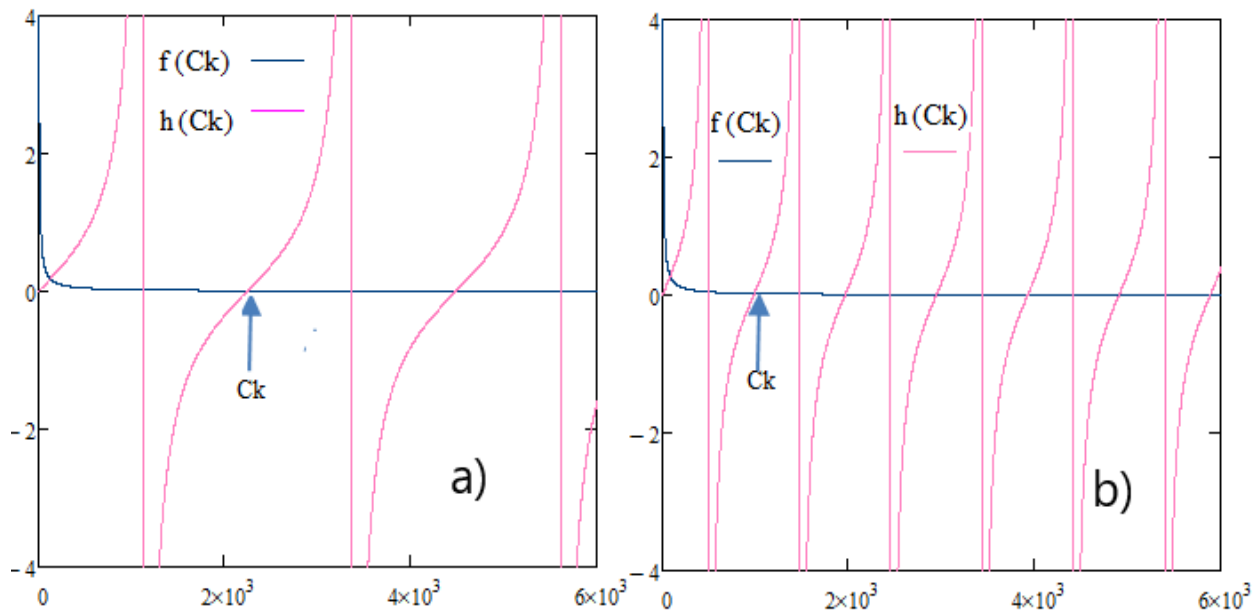
Figure 4: -Own values $S_g = 10^{3.0}$ cm/s, T = 333 K, a) g = 28 µm et b) g = 64 µm.

We find that the grain size (g) has a strong influence on the eigenvalues whatever the recombination rate at the grain interfaces and temperature. Figure 4.a was plotted for a grain size fixed at g = 28 µm while for figure 4.b, the grain size is fixed at 64 µm. We can see that for one interval in Figure 4.b, the number of C_k eigenvalues has doubled

compared with the interval in Figure 4.a. We have therefore plotted the eigenvalues associated with the grain sizes used in this work. The results are given in Table 3.

Table 3: -Own values $S_g = 10^{3.0}$ cm/s, T = 333 K.

Size (μm)	Own values $C_k = C_i$(/cm);k= 0, 1, 2, 3, 4				
10	179,600	3317,000	6619,000	9928,000	13230,000
28	127,613	2251,000	4492,000	6735,000	8978,000
37	119,139	1708,000	3401,000	5098,000	6795,000
46	114,659	1376,000	2737,000	4101,000	5466,000
55	104,619	1152,000	2290,000	3430,000	4572,000
64	96,764	991,502	1968,000	2949,000	3929,000
73	90,397	870,450	1726,000	2585,000	3445,000
82	85,099	775,968	1537,000	2302,000	3067,000
91	80,599	700,171	1386,000	2075,000	2764,000
100	76,714	638,015	1262,000	1888,000	2516,000

Impact of the operating point on the relative density of minority electrons
The normalized excess minority electron density profile as a function of base penetration depth for short-circuit and open-circuit modes of operation is shown in Figure 5.
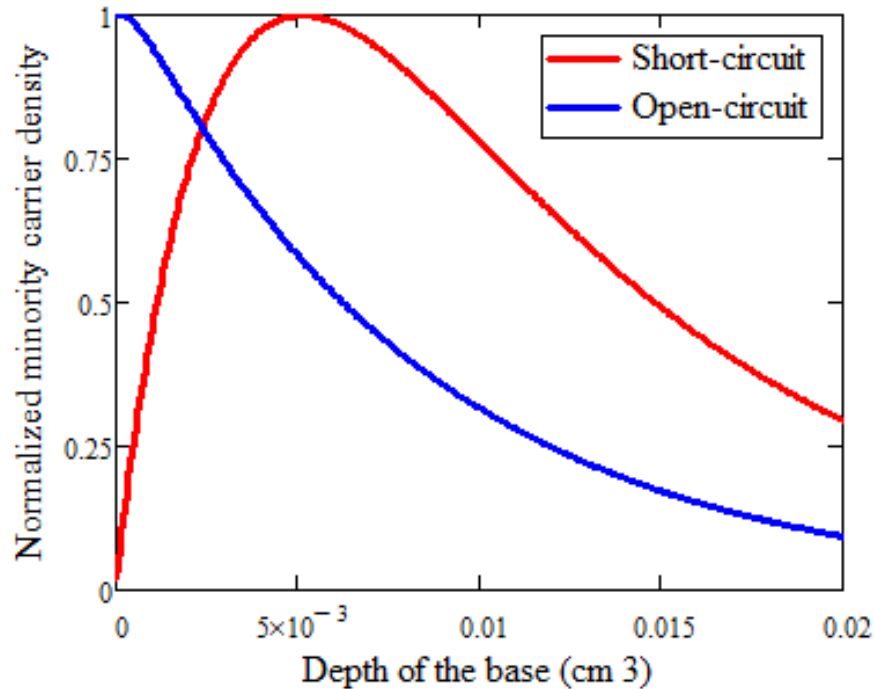
Figure 5:-Profile of the density of excess minority carriers in the normalised base as a function of the depth of the base for a temperature of T = 333K.

Xco (T, g) is the thickness of the transition region when the solar cell is operating in open-circuit mode.
Xcc (T, g) is the thickness of the transition region when the solar cell is operating in short-circuit mode.
The efficiency of the solar cell is expressed as the abscissas Xco (T, g) and Xcc (T, g) as[24]:

$$\eta(T,g) = 1 - \frac{Xco(T,g)}{Xcc(T,g)} \quad 20$$

The capacitance of a planar capacitor $C = \frac{\varepsilon \cdot S}{X}$ can be studied by comparing the maximum abscissae of two relative densities. Finding the performance of the capacitance is simplified to that of the abscissa Xcc(T, g), because the value of the abscissa Xco(T, g) is negligible compared with that of Xcc(T, g).

Cell capacity

The expression for capacity is obtained from the following relationship:

$$C(g,T,Sf) = \frac{\partial Q(g,T,Sf)}{\partial Vph(g,T,Sf)} \quad 21$$

Avec $\partial Q(g,T,Sf) = \partial \delta n(z=0,g,T,Sf) \quad 22$

$$C(g,T,Sf) = q \cdot \frac{\partial \delta n(z=0,g,T,Sf)}{\partial Vph(g,T,Sf)} \quad 23$$

By dividing the numerator and denominator of equation 23 by ∂Sf we obtain equation24:

$$C(g,T,Sf) = q \cdot \frac{\partial \delta n(z=0,g,T,Sf)}{\partial Sf} \cdot \frac{1}{\dfrac{\partial Vph(g,T,Sf)}{\partial Sf}} \quad 24$$

By solving equation 24, we obtained the expression for capacity given by equation 25:

$$C(g,T,Sf) = \frac{q \cdot n_i^2}{N_B \cdot V_T} + q \cdot \frac{\delta n(z=0,g,T,Sf)}{V_T} \quad 25$$

$$C(g,T,Sf) = C0(T) + Cd(g,T,Sf) \quad 26$$

C0(T)the cell's intrinsic capacity.

Cd(T, g)broadcasting capacity [14, 15].

Figure 6 shows the capacitance profile as a function of the diffusion rate at the n+/p face for a number of temperature values.
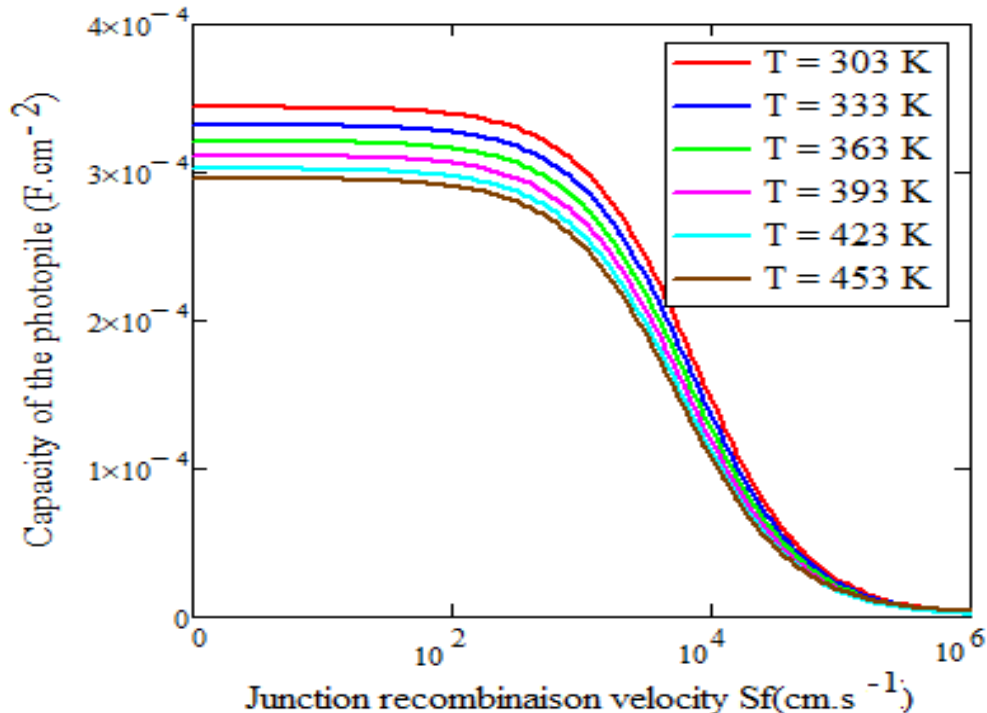
Figure 6: -Capacitance profile as a function of diffusion velocity across the transition zone for different temperatures: H = 200 μm, g = 28 μm, Sb = F (T), z = 0 μm.

These curves show three levels and decrease:

1. In an open circuit, the diffusion capacity is initially constant and maximum. This maximum diffusion capacity reflects the fact that there are few charge carriers in the p-zone crossing the junction. Hence a significant storage of charges in the space charge zone;

2. On short-circuit, the capacitance decreases and reaches its minimum. This decrease is due to the fact that a large number of minority charge carriers in excess in the base cross the emitter-base junction to participate in the generation of photocurrent. This leads to a depopulation of minority charge carriers in the storage area as the recombination rate at the junction increases;

3. A transient capacitance occurs between two operating points of the solar cell other than the open circuit and the short-circuit.

The effect of temperature is most visible in open circuit (SF < 10^2 cm/s). As the temperature increases, the Co(T) capacitance decreases and its thickness increases.As the operating point moves towards the short-circuit, the diffusion capacitance Cd(T, g) becomes small and its thickness increases. At this operating point, the capacitance can be associated with a large, temperature-dependent capacitor.

Figure 7 shows the capacitance profile as a function of temperature for different values of the grain size of a short-circuited solar cell.
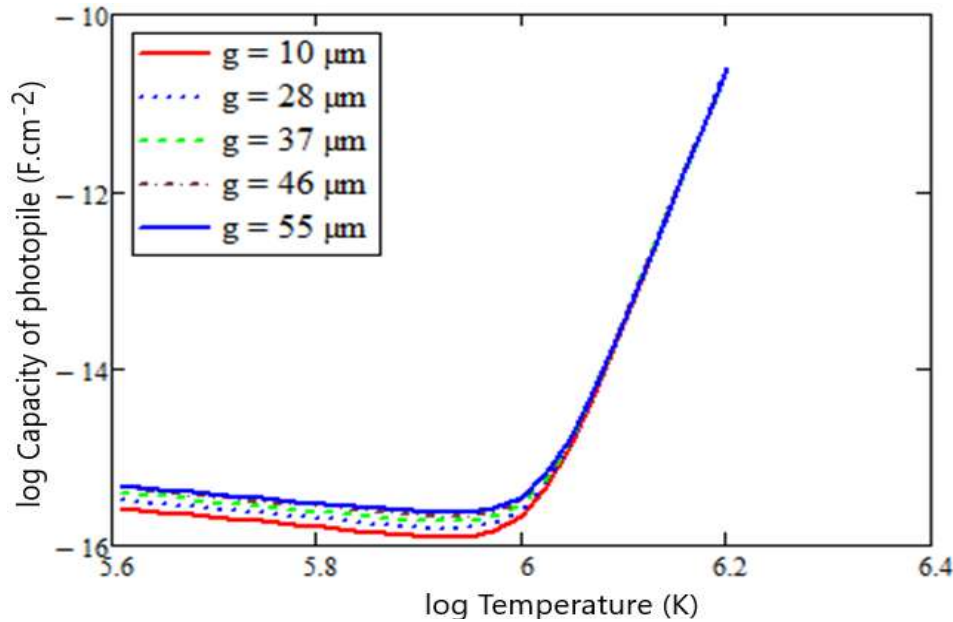
Figure 7: -Profile of logarithm of capacity as a function logarithm of temperature for different grain sizes: H = 120 µm, Sb = F (g), Sf = 6.10^6 cm. s^{-1}, z = 0 µm.

Within the limit of a minimum value Xcc(T, g) for the abscissa Topt (Topt = 383 K), the capacity of the solar cell decreases linearly with temperature. This is for temperatures below Topt. The extension of the transition zone is identical to the decrease in the cell capacity. Then we have a linear increase in capacity linked to the slope. This increase occurs at temperatures above Topt. This corresponds to a reduction in the thickness of the transition zone Xcc(T, g). The optimum temperature gives the best capacity. The projection of the point where the two tangents to the curve meet the temperature axis gives the optimum temperature. We also note that the short-circuit capacity of the solar cell decreases with smaller grain sizes.

The design of a theoretical model of the capacity of the solar cell using the profiles in Figure 7 is given in [25]:

$$C = \chi_g \cdot T^{\gamma_g} \quad 27$$

$\chi_g$is deduced from the intersection, it is equal to the capacity.
$\gamma_g$is the slope with Tγ homogeneous to capacity.

Table 4 shows the values for χ_g et $\gamma_g$obtained from figure 7.
Tableau 4: - Values of $\chi_g$andγ_g for different grain sizes.

Zone	g (µm)	χ_g (F/cm^2)	γ_g
T < Topt (g)	10	$1,32.10^{-7}$	-0,84
	28	$1,76.10^{-7}$	-0,84

	37	$1{,}93.10^{-7}$	-0,84
	46	$2{,}03.10^{-7}$	-0,84
	55	$2{,}03.10^{-7}$	-0,84
T > Topt (g)		$3{,}24.10^{-80}$	27,77

Conclusion: -

The study showed that the capacitance efficiency depends on Xcc(T, g), which is the area of extended space charge when the photocell is operated short-circuited. The expressions C0(T) and Cd(T, Sf, g) were determined from the composition of the photocell capacitance expression.

The evolution of capacity as a function of temperature for different grain sizes was used to determine the optimum Topt temperature that gives the best capacity.

When the temperature is below Topt, the capacity of the solar cell decreases linearly with temperature to a minimum abscissa corresponding to the value of Topt. This decrease is due to the extension of the thickness of the space charge zone Xcc(T, g).

For temperatures above Topt, the capacitance increases linearly whatever the grain size. This causes the thickness of the space charge zone Xcc(T, g) to shrink.

On the basis of this study, we modelled the capacity of the solar cell with temperature for a very high value of the recombination rate at the n+/p side (Sf = 10^6 cm/s), which imposes the short-circuit condition.

References Bibliographics: -

[1] Diop Nafy, Dione Gilbert Ndiassé, Loum Khady, Thiame Moustapha, ElhevidLemrabottHabiboullah, SowOusmaneandSissoko Gregoire (2024). Intrinsic recombination velocity at (n+/p) junction and monochromatic recombination velocity at (p/p+) surface of (n+/p/p+) silicon solar cell under temperature, as appklied to optimize (p) base thickness. Journal of Chemicat, Biological and Physical Sciences, pp. 011- 029 https://doi:1024214/jcbps.C15.1.01129

[2] Massa. Samba. Diop, Hamet. Yoro. Ba, Ndeye. Thiam, Ibrahima. Diatta, Youssou. Traoré, Mamadou. Lamine. Ba, El. Sow, Oulimata. Mballo, Gregoire. Sissoko (2019). Surface Recombination concept as applied to determinate silicon solar cell base optimum thickness with doping level effect. World Journal of Condensed Matter Physics, 9, pp.102-111https://doi.org/10.4236/wjcmp.2019.94008

[3] Mats Rosling, Henry Bleichner, Måns Lundqvist, Edvard Nordlander (1992). A Novel Tehcnical for the Simultaneous Measurement of Ambipolar Carrier Lifetime and Diffusion Coefficient in Silicon pp1223-1227.https://doi.org/10.1016/0038-1101(92)90153-4

[4] Misiakos K., Wang C. H., Neugroschel A. and Lindholm F. A. Lindholm (1990). Similtaneous extraction of minoritycarrier parameters in crystalline semiconductors by lateral photocurren, J.Appl. Phys. 67(1): pp. 321-333.https://doi.org/10.1063/1.345256

[5] P. Würfel, T. Trupke, and T. Puzzer. (2007). Diffusion lengths of silicon solar cells from luminescence images. JOURNAL OF APPLIED PHYSICS 101, 123110, p.110-123http://jap.aip.org/jap/copyright.jsp

[6]. Moustapha. Thiame, A. Diene, B. Seibou, Cheick. Tidiane. Sarr, M. L. O. Cheikh, Ibrahima. Diatta, M. Dieye, Youssou. Traoré, Gregoire. Sissoko, (2017). 3D Study of a Bifacial Polycrystalline Silicon Solar Cell Back Surface Illuminated: Influence of Grain Size and Recombination Velocity, JSER. 4(1) pp 135-145.

[7]. Mbao O., Thiame M., LY I., Datta I., Diouf M. S., Traore Y., Ndiaye M. and Sissoko G., (2016). 3D Study of a Polycrystalline Bifacial Silicon Solar Cell, Illuminated Simultaneously by Both Sides: Grain Size and Recombination Velocity Influence. International Journal of Innovative Science, Engineering & Technology, Vol. 3 Issue 12, pp.152-162 http://www.ijiset.com

[8].Ly. H. D., Maiga A. S., Wereme A., Sissoko G., (2008). New Approach of Both Junction and Back Surface Recombination Velocity in a 3D Modelling Study of a Polycrystalline Silicon Solar Cell. Eur. Phys. J. Appl. Phys. 42, pp.203-211 https://doi.org/10.1051/epjap:2008085

[9]Ousmane Diasse[1], Amadou Diao[1], Mamadou Wade[2], Marcel Sitor Diouf[1], Ibrahima Diatta[1], Richard Mane[1], Youssou Traore[1], Gregoire Sissoko[1], (2018). Back Surface Recombination Velocity Modeling in White Biased Silicon Solar Cell Under Steady State. J. Mod. Phys. 9, pp.189-201.**DOI:** 10.4236/jmp.2018.92012

[10] Moussa Ibra Ngom, Gilbert Ndiassé Dione, Khady Loum, Moustapha Thiame, LemrabottHabiboullahElhevid and Gregoire Sissoko (2024). Influence du champ magnetique et de la profondeur de la base sur la puissance et le rendementobtenus d'une photopile (N+/P) au silicium a jonctionsverticalesconnectees en parallele sous eclairementpolychromatique en regime statiqueInt.J.Adv.Res. 12(11), pp. 1300 – 1311 http://dx.doi.org/10.21474/IJAR01/19945

[11] KossoAtoumane Mamadou Moustapha., Moustapha. Thiame, Youssou. Traore, Ibrahima. Diatta, Malick. Ndiaye,Lemrabott. Habiboullah, Ibrahima. Ly, Gregoire. Sissoko, (2018). 3D Study of a Silicon Solar Cell under Constant Monochromatic Illumination: Influence of Both, Temperature and Magnetic Field. Journal of Scientific and Engineering Research, 5(7), pp.259-269online http://www.jsaer.com

[12] Richar. Mané, Hawa. Ly. Diallo, Hamet. Yoro. Ba, Ibrahima. Diatta, Youssou. Traoré, Cheick. Tidiane. Sarr and Gregoire.Sissoko, (2018), Influence of both magnetic field and temperature on silicon solar cell photogenerated current, Journal of scientific and engineering research, pp. 2394-2630

[13] Moctar OuldNouh Mohamed Mohamed[1], O Sow[2], Sega Gueye[1], Youssou Traore[1], Ibrahima Diatta[1], Amary Thiam[1], Amadou Mamour Ba[1], Richard Mane[1], Ibrahima Ly[3], Gregoire Sissoko[1], (2019), Influence of Both Magnetic Field and Temperature on Silicon Solar Cell Base Optimum Thickness Determination, Journal of modern physics, pp.1596-1605
DOI: 10.4236/jmp.2019.1013105

[14] Ibrahima Diatta, Issa Diagne, Cheikh Sarr, Khady Faye, Mor Ndiaye, and Grégoire Sissoko (2016) Silicon Solar Cell Capacitance: Influence of Both Temperature and Wavelength IPASJ I international Journal of Computer Science (IIJCS) pp 1-8.http://www.ipasj.org/IIJCS/IIJCS.htm

[15] Ibrahima Diatta[1], Ibrahima Ly[2], Mamadou Wade[2], Marcel Sitor Diouf[1], Senghane Mbodji[3], Grégoire Sissoko[1], (2016). Temperature Effect of Capacitance Silicon Solar Cell under Constant White Biased Light, World Journal of Condensed Matter Physics, 6; pp.261-268
ID:70063,8 pages10.4236/wjcmp.2016.63024

[16] **Marcel. Sitor. Diouf, Ibrahima. Gaye, A. Thiam, M. F. Mb. Fall, Ibrahima. Ly, Gregoire. Sissoko (2014)** Junction Recombination Velocity Induced Open CircuitVoltageFor A Silicon Solar Cell Under External Electric Field, Current Trends in Technology and Science, pp.372-375

[17] Ba M. L., Thiam, N., Thiame M., Traore Y., Diop M. S., Ba M., Sarr C. T., Wade M., and Sissoko G., (2019), Base Thickness Optimization of a (n+-p-p+) Silicon Solar Cell in Static Mode under Irradiation of Charged Particles. Journal of El ectromagnetic Analysis and Appl ications, 11, pp. 173-185. https://doi.org/10.4236/jemaa.2019.1110012

[18] SowO., Ba M. L., Ba H. Y., El Moujtaba M. A. O., Traore Y., Diop M. S., Wade M., Sissoko G., (2019), Shunt Resistance Determination in a SiliconSolar Cell: Effect of Flow Irradiation Energy and Base Thickness, Journal of electromagnetic Analysis and Application, pp.203-216

[19] Nzonzolo, D., Lilonga-Boyenga, Sissoko, G. (2014) Illumination Level Effects on Macroscopic Parameters of a Bifacial Solar Cell. Energy and Power Engineering, 6, pp25-36.

[20]. Dhariwal S. R., (1988). Photocurrent and Photovoltage from Polycrystalline p-n Junction Solar Cells Solar Cells, Vol.25. pp 223-233.

[21] Rauschenbach, H.S., Solar Cell Array Design Handbook. The Principles and Technology of Photovoltaic Energy Conversion (Van Nostrand Reinhold Ltd., New York, 1980)

[22]. Dugas J., (1994). 3D Modelling of a Reverse Cell Made with Improved Multicrystalline Silicon Wafers. Solar Energy Materials and Solar Cells 32, pp.71-88.

[23]. Sissoko G., Nanema E., Correa A., Adj M., Ndiaye A.L., Diarra M.N., (1998). Recombination Parameters Measurement in Double Sided Surface Field Solar Cell Proceedings of World Renewable Energy Conference, Florence–Italy, pp.1856-1859.

[24] Yaron, G. and Bentchkowsky, D.F. (1980) Capacitance Voltage Characterization of Poly Si-SiO2-Si Structures. Solid-State Electronics, **23**, pp.433-439.
http://dx.doi.org/10.1016/0038-1101(80)90078-7

[25] Thurmond, C.D. (1975) The Standard Thermodynamic Functions for the Formation of Electron and Hole in Ge, Si, GaAs and GaP. Journal of the Electrochemical Society, **122**, pp.133-141.
http://dx.doi.org/10.1149/1.2134410.